Cent. Eur. J. Phys. • 10(2) • 2012 • 492-499
DOI: 10.2478/s11534-011-0103-7

VERSITA

Central European Journal of **Physics**

EPR and optical properties of $KYb(WO_4)_2$ and $KTb_{0.2}Yb_{0.8}(WO_4)_2$ single crystals*

Research Article

Slawomir M. Kaczmarek[1†], Lucyna Macalik[2], Hubert Fuks[1], Grzegorz Leniec[1], Tomasz Skibiński[1], Jerzy Hanuza[2]

1 *Institute of Physics, Faculty of Mechanical Engineering and Mechatronics, West Pomeranian University of Technology Al. Piastow 48, 70-311 Szczecin, Poland*

2 *Institute of Low Temperature and Structure Research, PAS, P. Nr 1414, 50-950 Wrocław 2, Poland*

Received 24 September 2011; accepted 28 October 2011

Abstract: Well oriented $KYb(WO_4)_2$ and $KTb_{0.2}Yb_{0.8}(WO_4)_2$ single crystals have been investigated for their magnetic and optical properties using the Raman and EPR techniques. The registered EPR signal is dominated by three lines ascribed to ytterbium ions: one main and two satellites. Tb ions, although non-paramagnetic, distinctly modify magnetic properties of the $KYb(WO_4)_2$ single crystal. Basic parameters of the spin Hamiltonian, including Zeeman and hyperfine terms (**g** and **A** matrices) as well the spatial orientation between principal and crystallographic axes systems were determined for both crystals.

PACS (2008): 42., 42.55.-f, 42.70.-a

Keywords: EPR • single crystal • Ytterbium • Raman

1. Introduction

Physical properties of alkali-rare earth double tungstates result from the competition between spin-spin, electron-phonon, and magneto-elastic interactions. They determine the variety of magnetic, electronic, and crystallographic structures in such systems [1, 2]. The luminescence properties of rare earth (RE) double tungstates are closely connected with 4f-4f transitions and may be controlled by tuning the chemical and physical interactions. $KYb(WO_4)_2$ and $KTb(WO_4)_2$ crystals are isomorphous, crystallizing in monoclinic space group. They are applied as emitting materials for laser purposes [3, 4]. They differ, nevertheless, by magnetic properties. To check it clearly one can investigate mixed $KTb_xYb_{1-x}(WO_4)_2$ crystal. According to the crystal structure, two kinds of paramagnetic centers could nominally exist in all the above crystals: RE^{3+} ions with C_2 or lower point symmetry, located at distorted dodecahedra, and/or, reduced transition metal Me^{5+} ions located at tetrahedral or octahedral sites. The Electron Paramagnetic Resonance (EPR) technique is very useful for the determination of both the site symmetry and kind of magnetic interaction in crystals and powders. Using this technique, Yb^{3+} ions doped in $KY(WO_4)_2$ were

*presented at the 3rd International Workshop on Advanced Spectroscopy and Optical Materials, July 17-22, 2011, Gdańsk, Poland

†E-mail: skaczmarek@zut.edu.pl

previously investigated by Prokhorov *et al.* [5], whereas the dense magnetic system in a $KYb(WO_4)_2$ single crystal was analyzed by Pujol *et al.* [6] and recently by Borowiec *et al.* [1]. In the present work, we have examined a $KYb(WO_4)_2$ single crystal obtained by the method described by Borisov, Klevtsova [7]. Additionally, we have investigated a $KTb_{0.2}Yb_{0.8}(WO_4)_2$ single crystal, where introduction of diamagnetic dopant, such as Tb, could additionally affect the magnetic system and optical properties of the material.

2. Experimental setup

Single crystals of the double potassium ytterbium and terbium ytterbium tungstates were grown by the thermal method developed by Borisov and Klevstova [7] and Klevtsov *et al.* [8]. The cooling rate was 2°C per hour and the obtained crystals were transparent and of good optical quality. The samples were checked for purity by using X-ray powder diffraction. Room temperature Raman spectra were recorded using a JOBIN-YVON RAMANOR U-1000 spectrometer. Excitation was performed by 514.53 nm line of an SP Stabilize 201b argon laser. A CCD camera detection was used. The resolution was 2 cm^{-1}. EPR spectra of $KYb(WO_4)_2$ and $KTb_{0.2}Yb_{0.8}(WO_4)_2$ single crystals were recorded on a conventional X-band Bruker ELEXSYS E 500 CW-spectrometer operating at 9.5 GHz with 100 kHz magnetic field modulation. The first derivative of the powder absorption spectra has been recorded as a function of the applied magnetic field. Temperature and angular dependences of the EPR spectra of the samples in the 4-300 K temperature range were recorded using an Oxford Instruments ESP nitrogen-flow cryostat. The crystals were mounted in a resonance chamber and rotated around three laboratory chosen perpendicular axes connected with crystallographic directions: *a*, *b* and c^*, where the c^* axis in a monoclinic $KYb(WO_4)_2$ system is defined as being perpendicular to *a*- and *b*- crystallographic directions. To calculate spin Hamiltonian parameters, EPR-NMR program was applied [9].

3. Results and discussion

3.1. Crystal structure and vibrational characteristics. Raman spectra.

The $KYb(WO_4)_2$ and $KTb_{0.2}Yb_{0.8}(WO_4)_2$ single crystals crystallize in the monoclinic space group $C2/c \equiv C_{2h}^6$ (Z=4) with unit cell parameters obtained for $KYb(WO_4)_2$: a = 10.60 Å, b = 10.27 Å, c = 7.505 Å, β = 130.45°[5, 6].

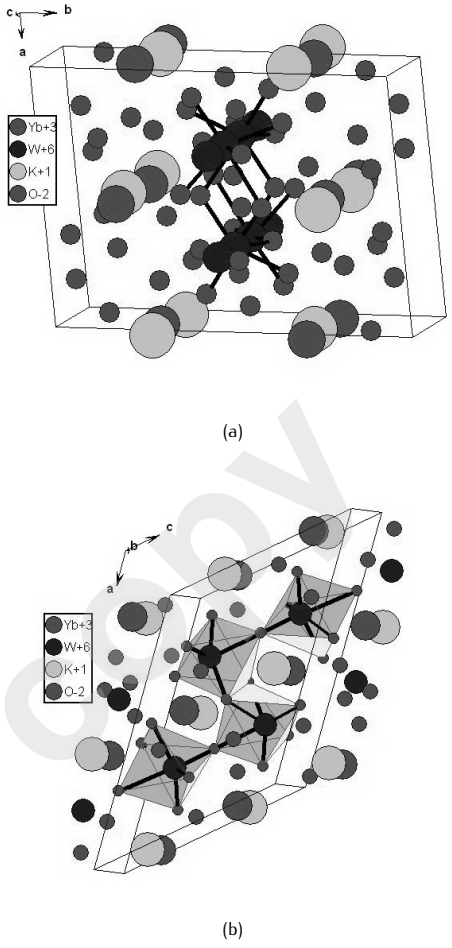

Figure 1. The crystal structure of $KYb(WO_4)_2$ in the *ab* (a) and *ac* (b) plane. W-O bonds are shown as thick lines (a) and polyhedra are added (b) to present the octahedral coordination of W atoms and the single and double oxygen bridges.

Tungsten and oxygen atoms occupy the 8f positions, forming a six-coordinated polyhedron of C_1 symmetry. The potassium and ytterbium/terbium atoms form twelve- and eight-coordinated oxygen polyhedra, respectively and they are placed at the 4e positions of C_2 symmetry. In Fig.1 the crystal structure of the unit cell in the *ab* and *ac* plane is presented.

Raman spectra of the $KYb(WO_4)_2$ crystal were reported elsewhere [10]. Polarized Raman spectra of $KTb_{0.2}Yb_{0.8}(WO_4)_2$ are presented in Figs 2, 3. The orientation of the crystal was realised using an X-ray method and the quality of polarizers was high, although the crystal was cut in that manner where all angles were equal to 90°. The following relation between the crystallographic *x*, *y*, *z* and optical *a*, *b*, *c* directions exists. *x* *a*; *y* *b*

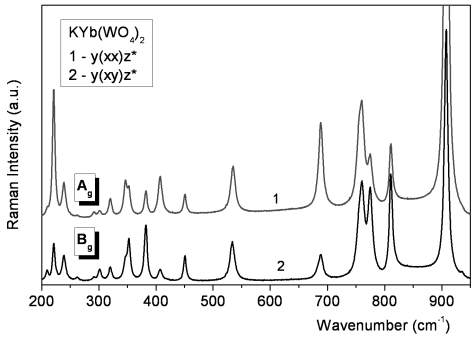

(a)

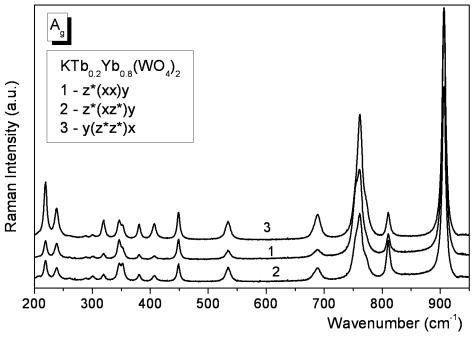

(b)

Figure 2. Polarized Raman spectra (A_g mode) of the of $KYb(WO_4)_2$ and $KTb_{0.2}Yb_{0.8}(WO_4)_2$ crystal (the following relation between the crystallographic *x*, *y*, *z* and optical *a*, *b*, *c* directions exists. *x* *a*; *y* *b* and *z** *c*; $\langle \beta(x,z) = 130°$, $\langle \beta(x,z^*) = 90°$).

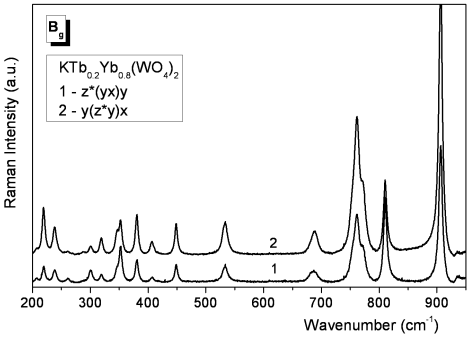

(a)

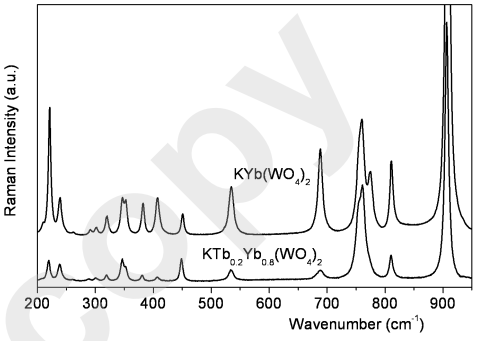

(b)

Figure 3. Bg mode of polarized Raman spectra of $KTb_{0.2}Yb_{0.8}(WO_4)_2$ crystal and the comparison of Raman spectra of $KYb(WO_4)_2$ and $KTb_{0.2}Yb_{0.8}(WO_4)_2$ crystals.

and z^* c; $\langle \beta(x,z) = 130°$, $\langle \beta(x,z^*) = 90°$. The Raman active A_g modes were measured in $z^*(xx)y$, $z^*(xz^*)y$ and $y(z^*z^*)x$ geometry and B_g modes - in $z^*(yx)y$ and $y(z^*y)x$ geometry. The bands at about 760 cm^{-1} and 350 cm^{-1} are the most sensitive for the polarization. The discussion of Raman spectra and description of the external and internal modes was proposed based on our previous papers [10–12]. Our results coincide well with that of the Factor Group Analysis (FGA) for an $KYb(WO_4)_2$ crystal. The observed spectra show 12 A_g and 12 B_g internal modes of the oxygen polyhedra and is the same as that predicted for this crystal. There are some bands in the 450-700 cm^{-1} region that confirms the existence of the oxygen bridges. Vibrations of the double oxygen bridge are characterised by six normal modes , that are assigned to the respective vibrational bands at 907, 760, 690, 535, 449 and 300 cm^{-1} for A_g, and at 907, 772sh, 763, 689, 450 and 301 cm^{-1} for B_g spectra. For the single bridge bond system the A_g vibrational frequencies are observed at 811, 533 and 239 cm^{-1} and B_g - at 810, 534 and 239 cm^{-1}.

3.2. EPR properties

Figs 4 show temperature evolution of the EPR spectra for both crystals. The spectra consist of one intense and asymmetric line, which asymmetry could result due to the fact that the observed EPR spectra are indeed a superposition of more than one resonance line. The asymmetry seems to be higher in the case of the $KYb(WO_4)_2$. EPR spectra of this crystal consist of at least four lines, three of them being assigned to even isotopes of $^{170}Yb^{3+}$ (central line) with no nuclear magnetic moments (I = 0, natural abundance 69.6) and two hyperfine transitions distributed about the central transition corresponding to nuclear spin I = 1/2 for ^{171}Yb isotope (natural abundance 14.3). Fourth line could be effectively a group of six hyperfine transitions distributed about the central transition corresponding to nuclear spin I = 5/2 for ^{173}Yb isotope (natural abundance 16.1, low field) [13]. The EPR spectrum of a $KTb_{0.2}Yb_{0.8}(WO_4)_2$ single crystal consists only of three former lines. Another reason of the EPR lines asymmetry in both cases could come from exchange or dipolar interactions between ytterbium ions, as is often observed

in a case of high concentration of paramagnetic dopants. Analysis of the shape fitting of the EPR resonance line registered for a $KYb(WO_4)_2$ crystal, revealed slight domination of the Gaussian shape over the Lorentzian one, indicating the domination of the dipolar nature of magnetic interactions between Yb^{3+} ions. This domination was found to be much higher for a $KTb_{0.2}Yb_{0.8}(WO_4)_2$ single crystal. The analysis of the EPR signal in both crystals originated from the supposition that the observed EPR signal is a composition of three lines i.e. even isotope $^{170}Yb^{3+}$ as a central line and two weaker satellite lines of ^{171}Yb isotope with I=1/2. The contributions to the overall shape of the EPR spectra from dipolar and exchange interactions were defined as follows: dipolar (Gaussian shape) - $c_i = 0$ and exchange (Lorentzian shape) - $c_i = 1$ (i=2 for main line and i=1, 3 for satellites):

$$EPR_{shape} = \sum_{i=1}^{3}[c_i L_i + (1 - c_i)G_i]. \quad (1)$$

As we found, a contribution of a given type of magnetic interaction to overall magnetic interactions (defined by c parameter) strongly depends on a temperature. It is clearly observed in Fig. 5a. In the case of a $KYb(WO_4)_2$ crystal, the absorption resonance lines broaden with increasing temperature (Fig. 5b), and at temperatures above 45 K the EPR spectrum is not visible, due to strong spin-phonon interactions (see Fig. 5b). As one can see from Fig. 5 the broadening is correlated with the domination of a given kind of magnetic interaction. For temperatures up to about 15 K, the linewidths stay constant (~120 mT). In this temperature range, almost the equivalence between two kinds of magnetic interactions is observed. Above 15 K, the contribution of dipole-dipole interaction in overall magnetic interactions decreases at the expense of exchange interactions. This change is almost linear vs. temperature for contribution parameter, c_2 (main line). Simultaneously, over 15 K, an exponential dependence emerges for the linewidth (Figs 5 a,b). The increase in a linewidth value seems to be attributed to shortening the spin-lattice relaxation time [14]. EPR spectrum of the $KTb_{0.2}Yb_{0.8}(WO_4)_2$ single crystal narrows for low temperatures up to 20 K and next broaden with increase of temperature (Fig. 5b), but is not visible over 35 K. The shape of the EPR line is also mixed (Lorentzian and Gaussian type; much more Gaussian as compared to $KYb(WO_4)_2$ case), so both kinds of interactions exist in the crystal, dipolar and exchange types, with prevailing contribution of the former one. As it results from Fig. 5, dipolar interactions dominate in a low temperature range (¡ 20 K), where a linewidth narrows. For higher temperatures the broadening of the EPR line is observed and simultaneous increase in the contribution of exchange interaction prevailing (linear change of the c-parameter with temperature increase) dipolar one. The dependence of the resonance line position as a function of rotation angle (roadmap), in general case , enables us to obtain some information about local symmetry of magnetic sites and their principal axes of spatial orientation. To reach this goal we analyzed the angular dependences of the resonance positions in all three rotation directions for both crystals. Yb^{3+} ion is a Kramer's type ion, in which case the crystal field of both crystals split energy levels giving only the lowest doublet populated, with effective spin S'=1/2. In this case the spin Hamiltonian could be described by the following equation:

$$H_s = \mu_B \mathbf{B}\mathbf{g}\mathbf{S}' + \mathbf{S}'\mathbf{A}\mathbf{I}, \quad (2)$$

where the first term represents the Zeeman interactions with an effective spin S'=1/2 and the second one is responsible for the hyperfine interactions; B - the external magnetic field, μ_B - the Bohr magneton, S and I - the electron and nuclear spin of the paramagnetic centres, respectively, **g** - tensor, that parametrizes the electronic Zeeman effect, and, **A** - hyperfine interaction tensor. The nuclear quadrupole term of odd Yb^{3+} isotopes is neglected in this case, because this kind of interaction we could not recognize in our spectra. According to well known reports [5, 6, 13], RE^{3+} ions doped to $KYb(WO_4)_2$ type double tungstates occupy the yttrium crystallographic position with C_2 point symmetry in eightfold coordinated irregular polyhedra. The principal magnetic axes system of RE^{3+} site generally do not coincide with crystallographic axes, but, due to characteristic spatial orientation of RE^{3+} polyhedra, two magnetic axes x and z are expected to lie in ac- plane, whereas a third axis, defined as y, coincides with b- crystallographic direction.

General formula describing the low symmetry case has the following form:

$$g_{eff}^2 = g_z^2 \cos^2\theta + g_x^2 \sin^2\theta \cos^2\varphi + g_y^2 \sin^2\theta \sin^2\varphi, \quad (3)$$

where: g_{eff} - is the experimental position of an EPR line, g_{xyz} - are the principal values of **g** matrix, θ and φ - are polar and azimuthal angles of the external magnetic field with respect to xyz axes system. In double tungstates under investigation, when y is parallel to b, formula (2) is significantly reduced, i.e. azimuthal angle φ is equal to zero. Taking this into account, the analysis of the roadmap in ac - plane should be useful in finding extreme positions of the resonance lines that determine the x - and z - magnetic axes.

Figs 6 a-c show an angular relation of the central resonance line (roadmaps) of ytterbium trivalent ion in a $KYb(WO_4)_2$ crystal in a, b, and c^* rotation mode i.e. when

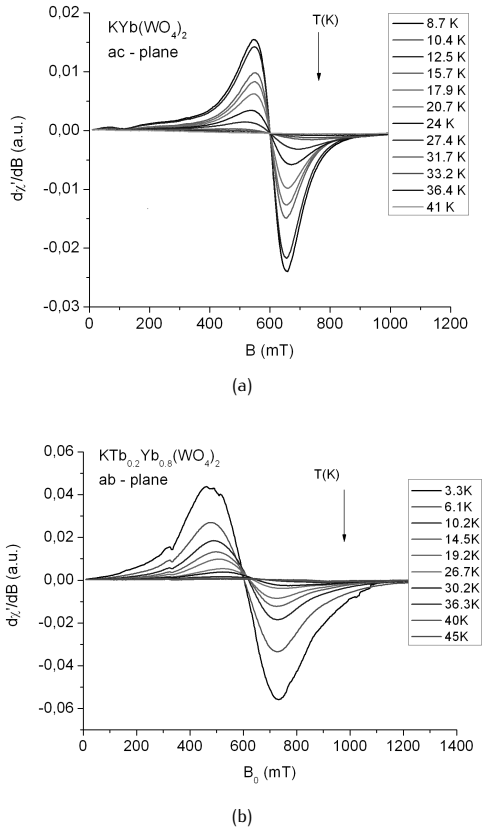

Figure 4. Temperature dependence of the EPR signal registered for $KYb(WO_4)_2$ single crystal in *ac*-plane (a) and $KTb_{0.2}Yb_{0.8}(WO_4)_2$ single crystal in *ab*-plane (b).

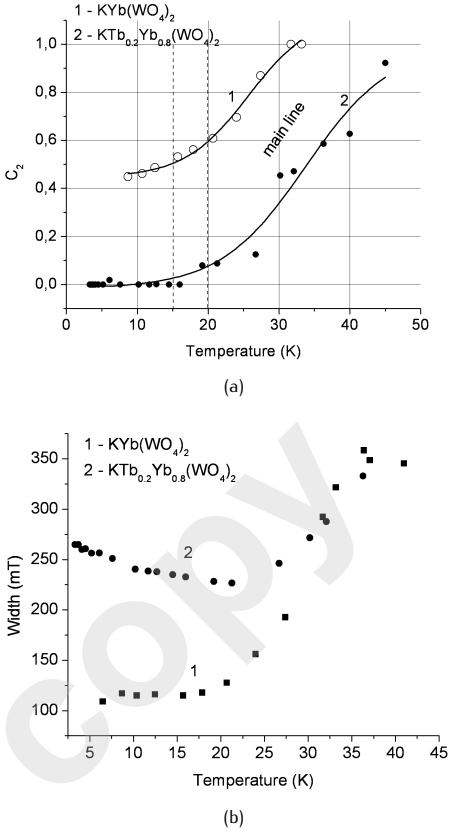

Figure 5. (a). Contributions of Gaussian (c_i = 0) and Lorentzian (c_i = 1) shapes to the overall shape of the EPR spectra for 1 - $KYb(WO_4)_2$ single crystal in *ac* plane and 2 - $KTb_{0.2}Yb_{0.8}(WO_4)_2$ in ab plane, (b). Linewidths of the EPR spectra registered for: 1 - $KYb(WO_4)_2$ single crystal in *ac* plane and 2 - $KTb_{0.2}Yb_{0.8}(WO_4)_2$ in *ab* plane.

magnetic field was operating in *bc*-, *ac*- and *ab*- plane, respectively. According to widely accepted definition, minimal value of magnetic resonance field indicates on the *z* direction, whereas position of a maximal field coincides with *x* direction of magnetic center (Fig. 6b). The EPR spectra of Yb^{3+}-doped host crystal at helium temperature should show at least single central line and also two satellite lines. Taking into account assumption on I=1/2 origin of the satellite lines, we performed a fitting of the Yb^{3+} lines in $KYb(WO_4)_2$ using EPR-NMR program [9]. The results of the fitting are presented in Figs. 6, 7, and 8 which show the resonance positions of Yb^{3+} main and satellite lines (dots) in *ab*- plane at 6.5 K for the $KTb_{0.2}Yb_{0.8}(WO_4)_2$2 single crystal as compared to the $KYb(WO_4)_2$ one. Having roadmaps in all three planes we employed the EPR-NMR program in order to find principal values of the **g** and **A** matrices more precisely. Solid lines in Figs. 6, 7, and 8a are results of a simulation by this program. As could be seen, simulated lines describe well enough experimental results in all planes for both crystals. Some discrepancy could appear due to difficulties in establishing a precise line position due to asymmetry of the EPR signal and its large linewidth. Principal values of the **g** and **A** matrices, calculated from the above fitting, are collected in Tab.1, including tilt angle between *z*- and *c**- axes (see also Fig. 5b). Similar crystal, $KYb(WO_4)_2$, but obtained by another method, was analyzed by Pujol *et al.* [6]. Values reported in the paper, also collected in Tab.1, seem to be enough good comparable with ours.

From the above figures and calculations, it results that doping with terbium ions changes magnetic properties of ytterbium ions in a $KYb(WO_4)_2$ crystal in a specific manner. Comparing both kinds of roadmaps presented in Figs 5, 6, and 7 one can conclude the resonance field of the EPR spectrum of the crystal doped with terbium shifts towards lower magnetic fields (Fig. 8b). It may result from lower concentration of ytterbium ions in case

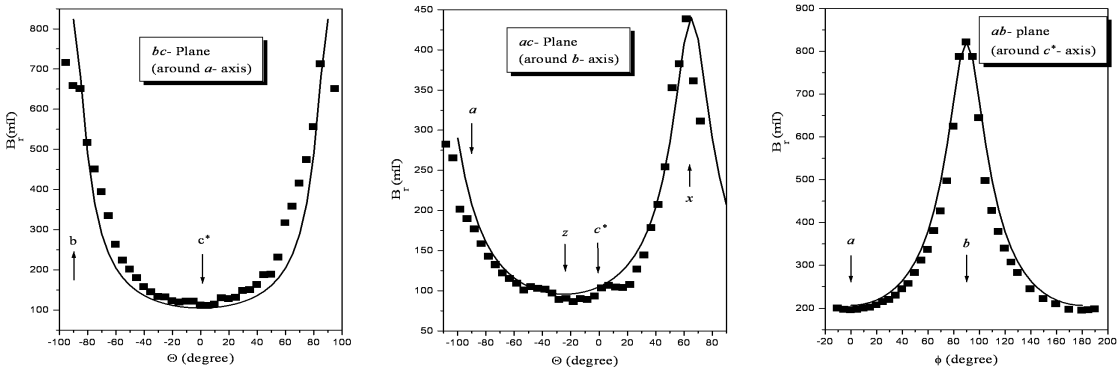

Figure 6. The resonance position of Yb^{3+} central line (squares) and the fitting function (solid lines) obtained by EPR-NMR simulation in *bc* -, *ac* - and *ab* - planes of $KYb(WO_4)_2$ crystal at 8.3 K. Horizontal values are polar or azimuthal angles of magnetic field in *abc** - axes system: (a) θ - relation, φ= 90°, (b) θ - relation, φ = 0°, (c) φ - relation, θ = 90°.

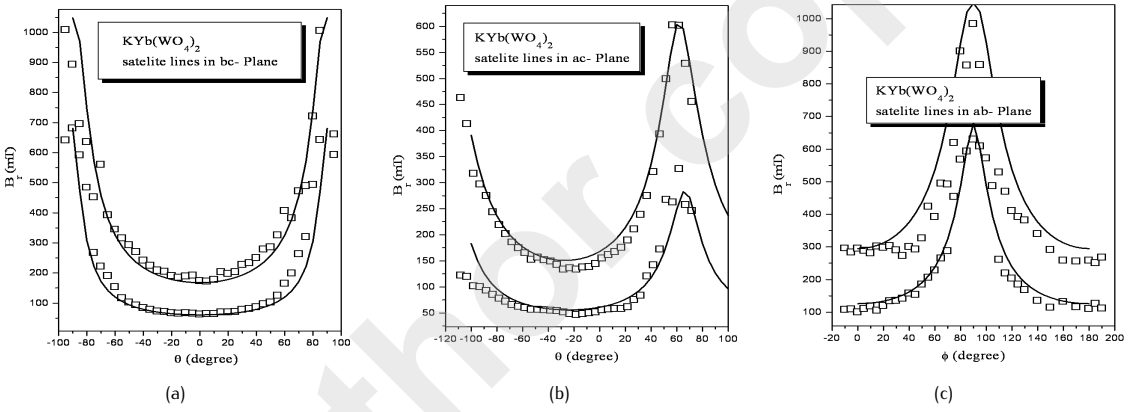

Figure 7. Experimental points (squares) and fitted curves (solid lines) of roadmaps of satellite lines for $KYb(WO_4)_2$ single crystal at 8.3 K, I=1/2 in case of: (a) *bc*-; (b). *ac*- and (c). *ab*- planes.

of $KTb_{0.2}Yb_{0.8}(WO_4)_2$. It may also indicate the influence of terbium ions on the distribution of ytterbium ions in $KTb_{0.2}Yb_{0.8}(WO_4)_2$ lattice. Comparing the **g** matrix calculated for $KTb_{0.2}Yb_{0.8}(WO_4)_2$ and $KYb(WO_4)_2$ crystals (Tab. 1) one can see that in a crystal with lower Yb^{3+} concentration the principal values of g_x and g_z are close to each other, whereas in the case of a dense ytterbium system g_x and g_y are close to each other. This means that in a crystal with low concentration of Yb^{3+} ions the anisotropy of the magnetic system is consistent with spatial orientation of C_2 yttrium polyhedra i.e. along the *y* axis. If we have a crystal with higher ytterbium doping, a more complex magnetic system is created with spatial symmetry perpendicular to *y* direction. The difference between the **g** matrices in dense and diluted ytterbium doped double tungstates is not confirmed in works [5] and [6] but was described by us in our novel work, being published soon. Additionally, according to our recent calculations, the tilt angle between *z*- and *c**- axes is very small in the case of a low concentration of Yb^{3+} ions (see Tab. 1), whereas the tilt reported in [5] and [6] is a significant one.

The magnetic interactions, as it results from the temperature dependence of the integral intensity (see Fig. 9) of main EPR line (double integral of the absorption EPR curve), are antiferromagnetic like in the case of a $KYb(WO_4)_2$ single crystal, and slightly ferromagnetic in the case of $KTb_{0.2}Yb_{0.8}(WO_4)_2$. It may indicate stronger separation of ytterbium ions each from another in the latter crystal. In this figure solid lines reflect Curie-Weiss law with Curie temperature equal to -1.5K (-1.05 [1]) and

Table 1. Principle values of g and A matrices and the tilt between *z*- and *c**- axes for $KYb(WO_4)_2$ and $KTb_{0.2}Yb_{0.8}(WO_4)_2$ single crystals.

Main EPR line				
$KYb(WO_4)_2$, this paper	$g_x = 1.532$	$g_y = 0.820$	$g_z = 7.058$	Tilt $zc^* = 25^0$
[6]	$g_x = 1.039$	$g_y = 0.997$	$g_z = 6.62$	Tilt $zc^* = 48^0$
$KTb_{0.2}Yb_{0.8}(WO_4)_2$	$g_x = 4.512$	$g_y = 0.772$	$g_z = 6.4410$	Tilt $zc^* = 2^0$
Satellite lines, parameters of A matrix $(cm)^{-1}$				
$KYb(WO_4)_2$	$A_x = 1700\times10^{-4}$	$A_y = 1100\times10^{-4}$	$A_z = 2900\times10^{-4}$	*ab*-plane
$KTb_{0.2}Yb_{0.8}(WO_4)_2$	$A_x = 2706\times10^{-4}$	$A_y = 2254\times10^{-4}$	$A_z = 3911\times10^{-4}$	*ab*-plane

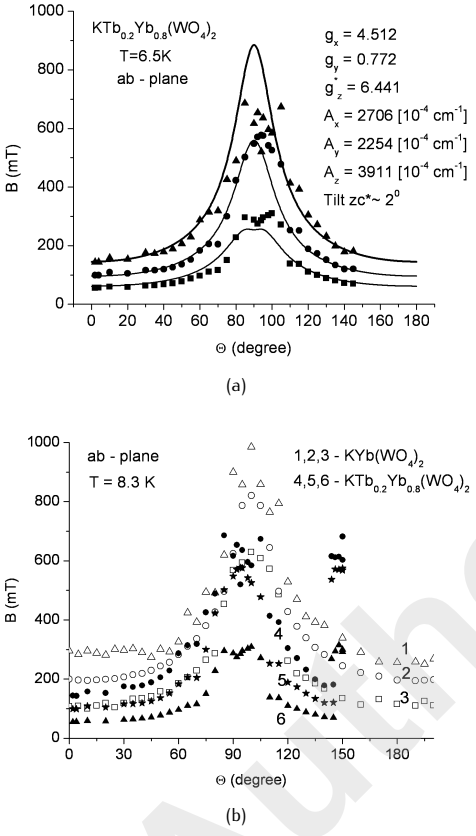

Figure 8. (a). The resonance positions of Yb^{3+} main and satellite lines (dots) and the fitting functions obtained by the EPR-NMR simulation (solid lines) for $KTb_{0.2}Yb_{0.8}(WO_4)_2$ crystals in *ab*- plane at 6.5 K, (b). Real roadmap of both investigated crystals in *ab* -plane at 8.3 K: 1-3 - $KYb(WO_4)_2$, 4-6 - $KTb_{0.2}Yb_{0.8}(WO_4)_2$.

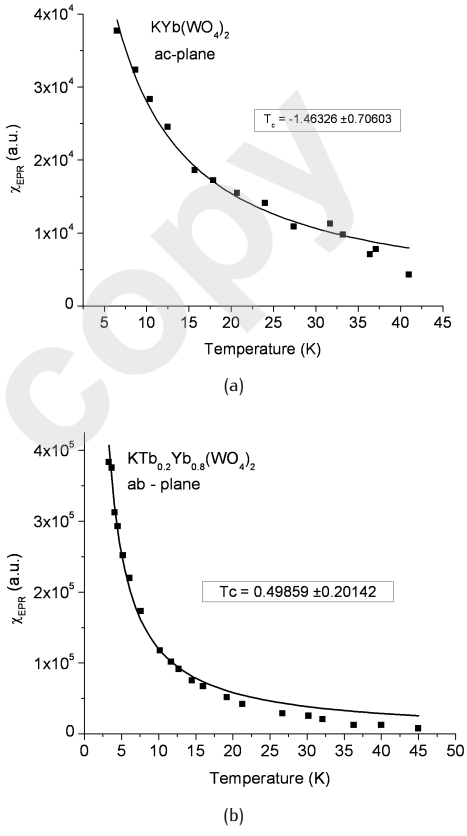

Figure 9. Temperature dependence of the integral intensity χ_{EPR} of the central EPR line for (a). $KYb(WO_4)_2$ in *ac*- plane, and, (b). $KTb_{0.2}Yb_{0.8}(WO_4)_2$ in *ab*- plane. T_c - Curie-Weiss temperature, $\chi_{EPR} = C/(T - T_c)$.

0.5 K for the former and latter crystals, respectively. The features agree well with ones derived by Borowiec *et al.* [1].

4. Conclusions

Raman spectra of the $KYb(WO_4)_2$ and $KTb_{0.2}Yb_{0.8}(WO_4)_2$ single crystals coincide well with that of the FGA for a $KYb(WO_4)_2$ crystal. Paramagnetic ytterbium ions replacing diamagnetic Y^{3+} ions in $KY(WO_4)_2$ matrix show strong anisotropy being dependent on the concentration of Yb^{3+} ions. This anisotropy (also asymmetry of the EPR line) may be due to strong hyperfine interactions and spin-

spin interactions (magnetic dipolar and exchange). The anisotropy decreases when a $KYb(WO_4)_2$ crystal is doped with diamagnetic terbium ions. Doping with diamagnetic ions may lead to a change in a distribution of ytterbium ions in the $KYb(WO_4)_2$ matrix. It may lead also to a change in a type of magnetic interaction by separating the ytterbium ions from each other. This change is strongly dependent on a temperature.

5. Acknowledgements

The authors acknowledge Prof. J. Baran for the possibility and help of carrying out the Raman measurements.

References

[1] M.T. Borowiec et al., Physica B 405, 4886 (2010)
[2] L. Macalik et al., Journal of Molecular Structure 450, 179 (1998)
[3] P. Klopp et al., Appl. Phys. B 74, 185 (2002)
[4] W. Strek, A. Bednarkiewicz, P.J. Deren, Journal of Luminescence 92, 229 (2001)
[5] A.D. Prokhorov et al., Eur. Phys. J. B 55, 389 (2007)
[6] M.C. Pujol et al., Physica B 388, 257 (2007)
[7] S. V. Borisov, R. F. Klevtsova, Kristallografiya 13, 517 (1968)
[8] P. V. Klevtsov, L. P. Kozeeva, L. Yu. Kharchenko, Kristallografiya 20, 1210 (1975)
[9] M. J. Mombourquette, J.A. Weil, D.G. McGavin, EPR-NMR User's Manual, Department of Chemistry, University of Saskatchewan, Saskatoon, SK, Canada (1999)
[10] L. Macalik et al., J. Lumin. 79, 9 (1998)
[11] J. Hanuza and L. Macalik, Spectrochim. Acta A 43A, 361 (1987)
[12] L. Macalik, J. Hanuza and A.A. Kaminskii, J. Molecular Struct. 555, 289 (2000)
[13] A. Abragam, B. Bleaney, Electron Paramgnetic Resonance of Transitions Ions, (Dover, New York, 1986)
[14] A.D. Prokhorov et al., Physica B 403, 3174 (2008)